

Performance Evaluation of a Parallel Cantilever Biaxial Micropositioning Stage

Edward Amatucci, Nicholas G. Dagalak, John A. Kramar, and Fredric E. Scire
National Institute of Standards and Technology
Gaithersburg, Maryland 20899

1. System Overview

The phenomenal growth of opto-electronic manufacturing and future applications in micro and nano manufacturing has raised the need for low-cost high performance micro-positioners. The National Institute of Standards and Technology (NIST) Advanced Technology Program (ATP) funded a team of NIST scientists and engineers to address the performance, testing and calibration needs of micropositioners. As a result of this effort various performance testing and calibration techniques are being developed on a new generation of micro-positioners with low crosstalk, good lateral resolution and strong load capabilities for delicate sub-micron automated assembly and positioning applications. The Parallel Cantilever Biaxial Micropositioning Stage (Figure 1.) is composed of two piezo-electric translators (PZTs) with internal capacitance sensors, two flexure joint couplings, a monolithic mechanical flexure baseplate, two capacitance sensors measuring the inner stage motions, control software and supporting commercial electronics. Inspired from the PiezoFlex¹ Stage [1] which has only one cantilever flexure mechanism on each axis, this new micropositioning stage has a novel configuration and design in that it has two parallel sets of cantilever beam flexures. This design reduces crosstalk in the X and Y translations and creates motions that are more linear and independent from each other in the X and Y directions.

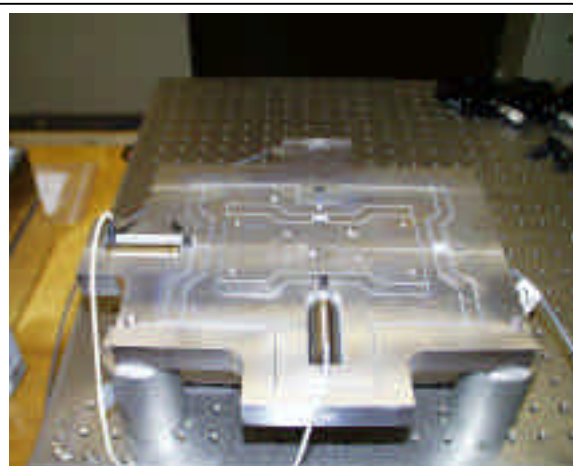


Figure 1. Parallel Cantilever 2D Micropositioning Stage

The other improvement includes the addition of sensors on axis with the actuator of the system. This is designed to reduce Abbe offset errors for precision measurement and control of the stage. Our new design has the potential to reduce the error caused by the rotation of the cantilever and also provide room for on-axis sensing of the moving x-y stage. It has two micro actuators and two sensors to directly monitor the actuator and stage motions respectively.

The other improvement includes the addition of sensors on axis with the actuator of the system. This is designed to reduce Abbe offset errors for precision measurement and control of the stage. Our new design has the potential to reduce the error caused by the rotation of the cantilever and also provide room for on-axis sensing of the moving x-y stage. It has two micro actuators and two sensors to directly monitor the actuator and stage motions respectively.

One of the more important performance characteristics of any planar micro-positioner is its angular cross talk error. All other errors can be compensated with the use of sensors and closed-loop feedback control. Correcting angular error cross talk can often require the use of expensive sensors and additional micro-positioners, which would then have to be connected in series with the planar micro-positioner to induce equal and opposite sign angular displacements. Our first generation micro-positioner has an unqualified (uncertainties yet to be determined) angular error of 0.3" to 0.4" ((1/12000)° to (1/9000)°).

2. Micro-positioner Controller

A simple motion controller of the micro-positioner has been developed. Figure 2 shows a schematic block diagram of the controller. The controller is running on a PC and issues motion commands to the controller of two piezoelectric PZT actuators, through a serial line connection. The actuators are Queens Gate (QG) 17 μ m capacity PZTs (Q1 and Q2 in Figure 2) and are mounted into machined holes within the structure of the micro-positioner. The actuators are equipped with embedded capacitive gauges, which measure the change in the length of the PZT stacks. This information is used by the QG controller to close the feedback loop. Our controller monitors and

¹ PiezoFlex is a trademark associated with Wye Creek Instruments design of a flexure stage. This and certain commercial products are identified in this paper to specify experimental procedures adequately. Such identification is not intended to imply recommendation or endorsement by the National Institute of Standards and Technology, nor is it intended to imply that the products identified are necessarily the best available for the purpose.

displays the actuator elongation information. The micro-positioner is equipped with two capacitive gauges described in the previous section (C1 and C2 in Figure 2), which monitor the absolute position of the moving stage

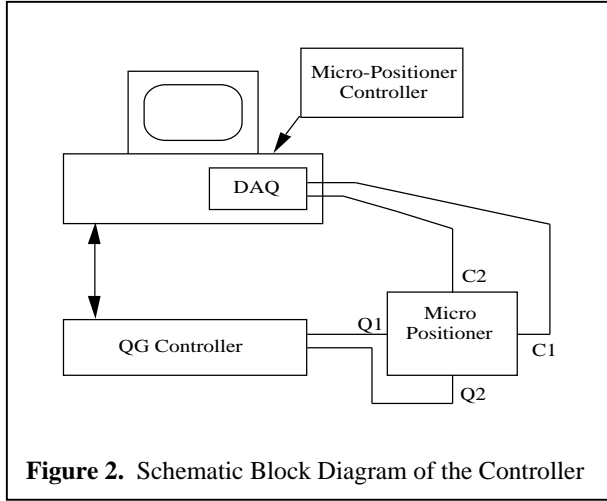


Figure 2. Schematic Block Diagram of the Controller

support the moving stage. K_c represents the stiffness of the coupling mechanism. B_{lo} , B_{li} and B_c represent the constants of dashpots, which model the losses due to structural damping and any other energy dissipating mechanism that might be used to dampen oscillations of the moving stage.

If X_i represents the input displacement generated by the actuator and X_s represents the displacement of the moving stage it is easy to show that the following relation is true:

$$X_s = GR X_i \quad (1)$$

where,

$$R = \frac{K_{li} K_c}{K_{li} K_{lo} + K_{li} K_c + K_{lo} K_c} \quad (2)$$

We call R the transmission ratio of the coupling mechanism and G the lever gain. It is obvious from eq. (2) that $R < 1$ since all stiffness values are positive. That means that the moving stage displacement will always be less than the displacement range of the actuator. R should be as large as possible to utilize as much of the available input displacement as possible. Increasing the stiffness K_c of the coupling mechanism will increase R . A very stiff coupler could transmit moments and shear forces that could destroy a piezoelectric stack actuator.

4. Square Trajectory Performance Test

During testing of a micro-positioner the coupling between the actuator and the cantilever beams was damaged. In one case the coupling was bent and in another case the clamping ball sheared through the shaft of the coupler. In both cases the damage was difficult to detect, because the deformation was small and hidden from view. To avoid operating under defective conditions a simple and fast square trajectory performance test was developed. This is a simple test that can easily spot problems with the operation of the micro-positioner. The micro-positioner is commanded to move its stage equal displacements sequentially along the X and Y orthogonal axes directions. The output displacement along the X and Y directions is measured, scaled and plotted on the controller monitor screen. The lengths of the sides of the trajectory plotted on the screen must be equal to the commanded displacement times the transmission ratio of the

along its two orthogonal axes. The outputs from these two gauges are digitized, by a data acquisition card (DAQ) and plotted on the control panel of the controller. The QG controller is not using these signals for feedback information. The operation of the controller is open loop in order not to mask the performance of the micro-positioner.

3. Mechanical Lumped Parameter Model

Figure 3 shows a simple mechanical lumped parameter model of the micro-positioner along a single axis direction.

In Figure 3, M_s represents the mass of the moving stage and M_c the mass of the actuator-to-stage coupling mechanism. K_{lo} and K_{li} are the stiffness of the two levers that

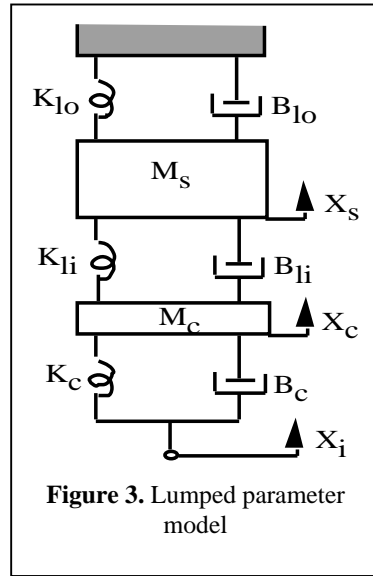


Figure 3. Lumped parameter model

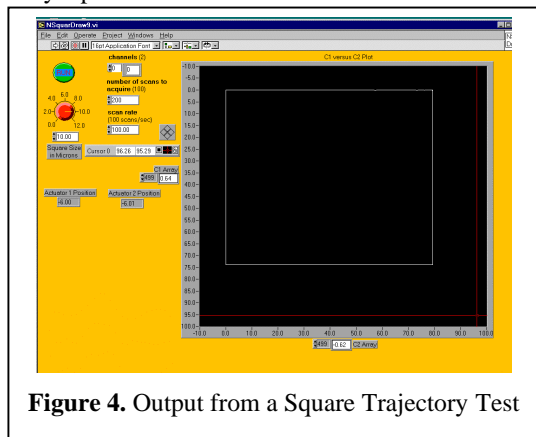


Figure 4. Output from a Square Trajectory Test

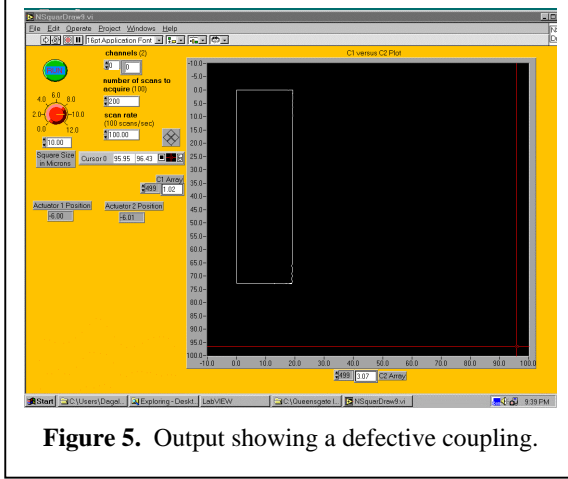


Figure 5. Output showing a defective coupling.

expected from the base line test. This defect would have gone undetected if it were not for the square trajectory test.

5. Calibration

Very often micro-positioners are run open loop without feedback position sensors. In that case it is

$$\begin{matrix}
 X_o & -\frac{L_{1x}}{2H_{1x}} & -\frac{L_{2x}}{2H_{2x}} & 0 & 0 & 0 & 0 & -\frac{L_{1y}}{2H_{1y}} & \frac{L_{2y}}{2H_{2y}} \\
 Y_o & 0 & 0 & -\frac{L_{1y}}{2H_{1y}} & -\frac{L_{2y}}{2H_{2y}} & -\frac{L_{1x}}{2H_{1x}} & \frac{L_{2x}}{2H_{2x}} & 0 & 0 \\
 \phi & \frac{L_{1x}}{W_x H_{1x}} & -\frac{L_{2x}}{W_x H_{2x}} & \frac{L_{1y}}{W_y H_{1y}} & -\frac{L_{2y}}{W_y H_{2y}} & 0 & 0 & 0 & 0
 \end{matrix}
 \begin{matrix}
 X_{1i} \\
 X_{2i} \\
 Y_{1i} \\
 Y_{2i} \\
 X^{2_{1i}} \\
 X^{2_{2i}} \\
 Y^{2_{1i}} \\
 Y^{2_{2i}}
 \end{matrix}$$

Figure 6. Kinematic model equations

important to perform a careful calibration in order to determine the correct command signals for the desired output position of the moving stage. One way to calibrate these devices is to develop a mathematical model of the kinematic mechanism, perform the proper experiments, and then use the results to estimate the parameters of the mathematical model. The model can then be used to solve the inverse kinematic

problem, to estimate the motion command signals that correspond to the desired positions of the moving stage.

Figure 6 shows the kinematic model equations of the parallel cantilever biaxial micro-positioner. X_i and Y_i are the input displacements generated by the actuators and X_o , Y_o , are the output displacements. ϕ is the yaw rotation angle of the moving stage. The subscripts 1 and 2 correspond to the individual levers for the cases where they are activated by separate actuators. The subscripts x and y correspond to the directions of the two orthogonal axes. L is the distance between the lever pivot point flexure and the flexure that transmits the force to the moving stage. H is the distance between the lever pivot point flexure and the flexure that transmits the force from the actuator to the lever. W is the distance between the two flexures that transmit forces to each side of the stage along the one axis direction. Figure 7 shows the dimensional symbols marked on a picture of the micro-positioner.

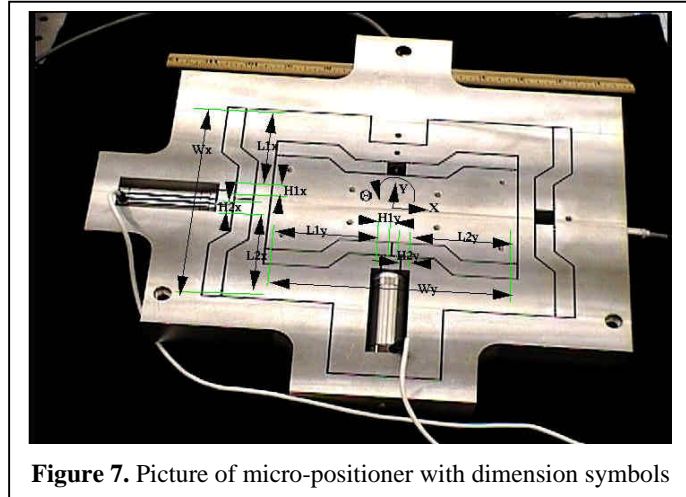


Figure 7. Picture of micro-positioner with dimension symbols

The accuracy of the calibration algorithm depends on several parameters. We are currently investigating the effects of the following: 1) the level of complexity of the mathematical model, such as the effect of non-linear terms

coupling times the micro-positioner gain. For example, if the commanded input displacement is 10 μm , the transmission ratio is 0.7, and the gain is 10, the measured output displacement would be 70 μm . This is a simple test to perform and can provide an easy measurement of the micro-positioner couplings transmission ratios. Figure 4 shows the output from such a test.

This type of test can be performed when the micro-positioner is in good operating condition and then used as a baseline to monitor the operation of the micro-positioner. Figure 5 shows the result from a test when one of the couplings of the micro-positioner was defective. This particular coupling was not capable of transmitting high actuation forces. Overloading or repeated rapid changes in the direction of motion resulted in deformation and slippage. As can be seen from Figure 5 the output displacement along axis #2 is much smaller than that

in the mathematical equations of Figure 6.; 2) the number and location of the calibration test positions; 3) the noise in the stage position measurement sensors; and 4) the curve fitting algorithm of the mathematical equations. The suitability of a calibration algorithm can be judged by its ability to predict experimental data. Figure 8 shows a plot of the magnitude of the calibration model vs. experimental x and y position error.

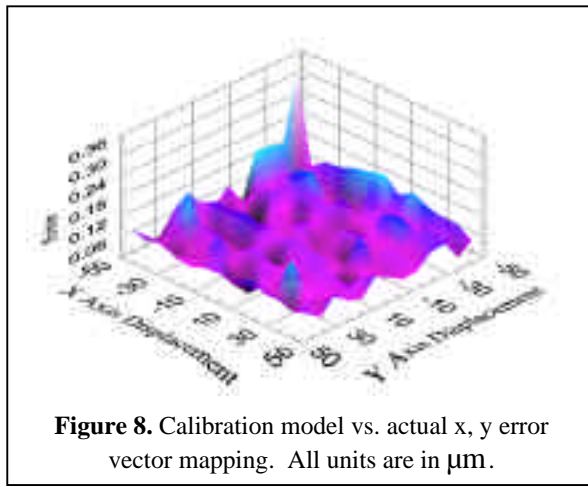


Figure 8. Calibration model vs. actual x, y error vector mapping. All units are in μm .

determined from one autocollimator's measurements. The yaw scale has been offset about its mean value for clarity. The yaw is approximately 0.3" or 0.4". Note that we are only showing the worst set of our data and also determined data for pitch, roll and yaw with both autocollimators. Bottom line, the cross couplings from these small yaw angles are going to be approximately 0.2 μm over the whole work zone. For small areas we will have excellent performance.

7. Conclusions

In conclusion, performance measures and calibration techniques used on the prototype designs are critical for industry to fabricate larger numbers of these devices. This will provide a low cost system backed by sound calibration, performance measures and design principals. Reduction in size can be accomplished with the use of special metals or composites and/or the use of special fabrication techniques and design modifications [2,3]. The durability of the stage will be enhanced with mechanical stops that will protect the flexure elements from being damaged from accidental abrupt contact by robotic end-effectors placing assembly components on the stage. Also, various configurations of this stage will be developed including a three, four and six axis version.

8. Acknowledgements

We would like to thank Dr. Lowell Howard, Dr. E. Clayton Teague, Jason Marcinkowski, James Gilsinn, Chris Nowakowski, Brian Weiss, and NCMS Optoelectronics Consortium Members for their contributions.

9. References

1. Scire, Fredric E., Teague, Clayton E., "Piezodriven 50- μm range stage with subnanometer resolution", *Rev.Sci.Instrum.*, 49(12), December 1978, pp. 1735-1739
2. Smith, S. T. and Chetwynd, D. G., "Foundations of Ultraprecision Mechanism Design", *Gordon and Breach Science Publishers*, 1992, Volume 2
3. Slocum, Alexander H., "Precision Machine Design", *Prentice-Hall, Inc.*, 1992, pp. 1-743

6. Roll-Pitch-Yaw Error Test

Two Elcomat autocollimators were employed with an optical square to provide simultaneous measurement of pitch, roll and yaw. Resolution of the Elcomat is at least 0.01". Accuracy is limited to perhaps an order of magnitude worse if care is not taken to enclose the optical beam path within a tube and average at least 20 s of data for each data point. By combining autocollimator measurements with microstage displacement measurements, straightness of travel may be estimated by using a numerical integration algorithm. A LabView program was written to move the stage through a serpentine pattern along a 10 x 10 matrix of positions. At each position, approximately 1000 autocollimator measurements were collected and averaged together. Figure 9 shows the result for yaw

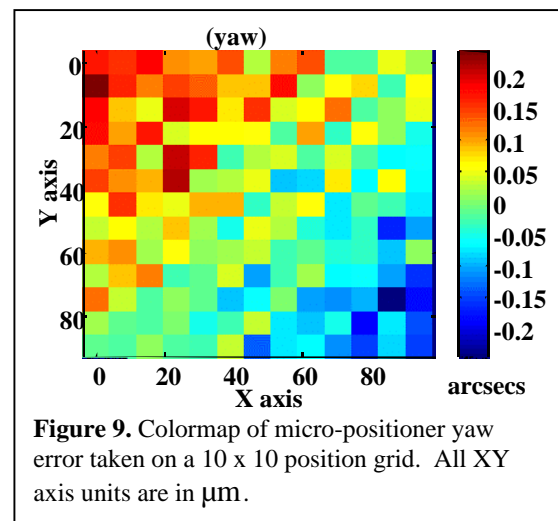


Figure 9. Colormap of micro-positioner yaw error taken on a 10 x 10 position grid. All XY axis units are in μm .